Symmetry of Model $N = 3$ for Graphene with Charged Pseudo-Excitons

Halina V. Grushevskaya[*] and George Krylov[†]

Physics Department, Belarusan State University,
4 Nezalezhnasti Ave., 220030 Minsk, BELARUS

V. A. Gaisyonok[‡]

National Institute of Higher Education, 15 Moskovskaya Str, 220007 Minsk, BELARUS

D. W. Serow[§]

Saint-Petersburg State Polytechnical University,
29 Politechnicheskaya Str, 195251 Saint-Petersburg, RUSSIA

A model $N = 3$ of graphene charge carriers has been proposed. Within the model the pseudo-helicity is determined by the exchange interaction for p_z -electrons. The symmetry properties of the model have been examined. It has been shown that the pseudo-helicity conservation law allows to explain experimental data on "moire" pattern and long spin relaxation time in graphene.

1. Introduction

The spin relaxation time is known to be a rather long for charge carriers in graphene [1]. The phenomenon of weak damping of spin correlations in graphene makes it promising for constructing quantum devices based on magnetoelectric effects in graphene monolayer [2]. Two facts are important for understanding this phenomenon, fist is that the spin relaxation is stipulated by magnetic moments scattering [2]. The second one is that main properties of charged carrier transport in graphene can be explained by Klein tunneling [6–8]. There exist several explanations of long spin relaxation time. A quantum mechanical Elliott—Yafet spin-flip mechanism [3, 4] and a resonant scattering mechanism with spin-flip exchange field [5] assume that the long time of spin relaxation is

connected with electron-hole pairs production. Theoretical description of such situations is difficult as it encounters the Klein paradox [9, 10] when unphysical states appear. The Klein paradox could be overcome by secondary quantization but in this case the concept of a single electron itself becomes meaningless. Inner discrepancy makes these models not predictive ones.

A Dyakonov–Perel mechanism [11] is a classical model where spin precession prevents the spin correlation relaxation. In quantum theory the precession corresponds to level splitting on sublevels with opposite spin directions (Zeeman effect). Quantization of the Dyakonov–Perel mechanism leads to oscillations between electron and hole state that is equivalent to electron-hole production process. Therefore after quantization the Dyakonov–Perel mechanism also suffers with the problem of Klein paradox.

Charge transport in pure graphene was considered in several papers on the basis of Boltzmann equation [12], Kubo formalism [13, 14] and quantum field theory [15]. Interactions

────────
[*]E-mail: `grushevskaja@bsu.by`
[†]E-mail: `krylov@bsu.by`
[‡]E-mail: `rector@nihe.by`
[§]E-mail: `dimusum@yandex.ru`

between single-particle excitations leading to appearance of charge carriers dynamical mass in graphene have been described by quantum electrodynamics methods in [16]. In [17] an excitonic coupling was considered in the form of non-charges exciton composed of electron and a hole; the approach was based on the gauge Eliashberg theory with a number of internal degrees of freedom $N = 2$ (physical flavors): pseudo-spin and pseudo-charge. The above-mentioned theories of charge carrier transport in graphene with pseudo-Dirac hamiltonian [18] give the value of dynamic (optical) low frequency conductivity $\sigma(\omega, \ k)$ equals $\pi e^2/(2h)$ for wave number k, vanishing in respect to frequency ω: $k \ll \omega$. Here e is the electron charge, h is the Planck constant.

Graphene belongs to strongly correlated many-body systems. We assume that the inclusion of only two-particle exciton pairing makes graphene monolayer description not complete and causes discrepancy of theoretical and experimental data on graphene charge carriers transport.

In this paper, we use the theory with $N = 3$, which implies the existence of a process of three-particle exciton pairing [19].

The goal of the paper is to derive an exchange operator in the relativistic gauge model $N = 3$ of graphene, symmetry properties of the model and to use them for explanation of experimental data on "moire" patterns and spin relaxation time.

2. Model of graphene charge carriers with the pseudo-spirality conservation law

Monatomic graphene layer of hexagonally packed carbon atoms, shown schematically in Fig. 1, is a material with a half-filled valence band. A distinctive feature of graphene band structure is the existence of Dirac cones in edges (valleys) K, K' of the Brillouin zone. In the paper these points are designated as Dirac points K_A, K_B.

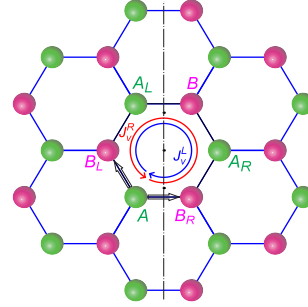According to Fig. 1 a particle can travel from node A to, for example, a node A_R through the

FIG. 1. Graphene lattice, comprised of two sublattice A and B. Right left valley currents J_v^R and J_v^L are shown as rounded curves with arrows. Double arrows from node A to node B_L and from A to B_R indicate clockwise and anti-clockwise directions. The axis of mirror reflection from A_R to B_L is marked by bar dotted line. (in color)

right B_R or left B_L nodes. Since the particle is symmetrical, the its description in the right and left reference frames have to be equivalent. Therefore the wave Ψ' of graphene has to be chosen in a Majorana form, which upper and lower spin components ψ', $\dot{\psi}'$ are transformed by left and right representations of the Lorenz group:

$$\Psi' = \begin{pmatrix} \psi'_\sigma \\ \dot{\psi}'_{-\sigma} \end{pmatrix} = \begin{pmatrix} e^{\frac{\kappa}{2}\vec{\sigma}\cdot\vec{n}}\psi_\sigma \\ e^{\frac{\kappa}{2}(-\vec{\sigma})\cdot\vec{n}}\dot{\psi}_{-\sigma} \end{pmatrix}. \quad (2.1)$$

The wave-function of a particle (in our case of electron-hole pair) $\widehat{\chi^\dagger_\sigma}(\vec{r}_A)|0, +\sigma\rangle$ located on the sublattice A, behaves as a component ψ_σ, and the wave-function of a particle $\widehat{\chi^\dagger_{-\sigma}}(\vec{r}_B)|0, -\sigma\rangle$, located on sublattice B, – as a component $\dot{\psi}_{-\sigma}$ of the bispinor (2.1).

Relativistic particles are characterized by helicity h which represents the projection of spin to the direction of motion [20]:

$$h \equiv \vec{p}\cdot\vec{S} = \frac{1}{2}p_i \begin{pmatrix} \sigma_i & 0 \\ 0 & \sigma_i \end{pmatrix} \quad (2.2)$$

where $\vec{S}$ is the spin operator, $\vec{\sigma}$ is a vector of Pauli matrices σ^i, $i = x, \ y$. In quantum relativistic field theory, the value of the helicity of a massless particle is preserved at the transition from one reference frame moving with velocity v_1, to another one moving with velocity v_2 [20, 21].

Let us denote $\vec{S}_{AB} = \hbar\vec{\sigma}_{AB}/2$ and $\vec{S}_{BA} = \hbar\vec{\sigma}_{BA}/2$ two-dimensional (2D) spin of quasi-particle in valleys K_A and K_B, respectively. Valley current J_v^R or J_v^L, on right $\{A \rightarrow B_R \rightarrow A_R \rightarrow B \rightarrow A_L \rightarrow B_L \rightarrow A\}$ or left $\{A \rightarrow B_L \rightarrow A_L \rightarrow B \rightarrow A_R \rightarrow B_R \rightarrow A\}$ closed contour in Fig. 1, is created by electron with pseudo-angular momentum $\vec{l}_{AB_R}$ and momentum $\vec{p}_{AB_R}$ or by electron with $\vec{l}_{AB_L}$ and $\vec{p}_{AB_L}$. Pseudo-helicity of bispinors (2.1), describing a particle right or left from lattice node A, is defined by the expressions which are analogous to (2.2):

$$h_{B_R A} \equiv \vec{p}_{AB_R} \cdot \vec{S}_{B_R A}, \qquad (2.3)$$

$$h_{B_L A} \equiv \vec{p}_{AB_L} \cdot \vec{S}_{B_L A}. \qquad (2.4)$$

Let us act by the parity operator P, which mirrors the bispinor (2.1) as $A \rightarrow B$ in respect to the center of inversion. Pseudo-helicity of the mirrored bispinor is defined by the expression

$$P h_{B_R A_R} P = h_{A_L B_L} = \vec{p}_{B_L A_L} \cdot \vec{S}_{A_L B_L}. \quad (2.5)$$

Due to the fact that valley momentum and pseudo-spin change signs: $\vec{p}_{A_L B_L} = -\vec{p}_{B_R A_R}$ and $\vec{S}_{A_L B_L} = -\vec{S}_{B_R A_R}$, pseudo-helicity h_{AB} does not change its value.

Pseudo-helicity h_{AB} is expressed through the projection $\tilde{\mathcal{M}}_{AB} = \vec{\sigma}_{BA} \cdot \left(\vec{l}_{AB} + \hbar\vec{\sigma}_{BA}/2\right)$ of total angular momentum on the direction of spin $\vec{\sigma}_{BA}$ as [22, 29]:

$$\vec{\sigma}_{BA} \cdot \vec{p}_{AB} = \sigma_{BA}^r \left(p_{r,BA} + \imath \frac{\tilde{\mathcal{M}}_{AB}}{r} - \hbar/2\right)$$

$$= \sigma_{BA}^r \left(p_{r,BA} + \imath \frac{\vec{\sigma}_{BA} \cdot \vec{l}_{AB}}{r}\right) \qquad (2.6)$$

where σ_{BA}^r and $p_{r,BA}$ is a radial components of spin and momentum respectively. According to (2.6) preudo-spin-orbital scalar $\vec{\sigma}_{BA} \cdot \vec{l}_{AB}$ describes the coupling (interaction) of spin with valley currents flowing along a closed loop in a clockwise or in opposite directions as shown in Fig. 1. Hence, there exists a preferred direction along which spin projection of bispinor (2.1) does not change after transition from one moving reference frame into another one. At this, the spin of a particle precesses and, respectively, the described transformation of the electrons and holes into each other in exciton is a pseudo-precession.

Thus, the coupling of pseudo-spin and valley currents stipulates the spin precession of current exciton charge carriers in graphene. In our model the orientation of non-equilibrium spin of the states of monolayer graphene in electromagnetic fields may be retained for a long time due to prohibition of change for exciton pseudo-helicity. Pseudo-precession is possible, if spins of p_z-electrons are anti-ordered (antiferromagnetic ordering). Therefore, the pseudo-spin precession of the exciton can be implemented through the exchange interaction. Further, let us find an exchange mechanism of strong correlations, leading to pseudo-precession.

3. Exchange operator for a system with a half-filled valence band

3.1. Procedure of the second quantization

In approximation of the Dirac–Hartree–Fock self-consistent field [22, 23], only valent electrons contribute to graphene Hamiltonian [19, 24–27]

$$H_D = \sum_{L=A,B} \sum_{i=1}^{N/2} \sum_{v=1}^{4} \left\{ c\vec{\alpha} \cdot \vec{p}_{i_L^v} + \beta m_e c^2 - \sum_{k=1}^{N} \frac{Ze^2}{|\vec{r}_{i_L^v} - \vec{R}_k|} + \sum_{L<L'=A,B} \sum_{i<j=1}^{N/2} \sum_{v'=1}^{4} \frac{e^2}{|\vec{r}_{i_L^v} - \vec{r}_{j_{L'}^{v'}}|} \right\}, \quad (3.1)$$

$$\vec{p} = -\imath\hbar\vec{\nabla}, \ \vec{\alpha} = \begin{pmatrix} 0 & \vec{\sigma} \\ \vec{\sigma} & 0 \end{pmatrix}, \ \beta = \begin{pmatrix} 1 & 0 \\ 0 & -1 \end{pmatrix}. (3.2)$$

Here $\vec{\alpha}$, β is a set 4×4 of Dirac matrices, $\vec{\sigma}$ is the set of 2×2 Pauli matrices, indices v and v' enumerate s-, p$_x$-, p$_y$ and p$_z$ electron orbitals, indices L, i and L', j enumerate sublattices and atoms within them respectively, $\vec{r}_{i_L^v}$ is the electron radius-vector, $\vec{R}_k$ is the radius-vector of k-th carbon atom without valent electrons (atomic core), $-Ze = -4e$ is the charge of the atomic core, e is the electron charge, m_e is the free electron mass, c is the speed of light.

We use the method of projection operators to secondary quantize the Hamiltonian (3.1). Density matrix $\hat{\rho}_{rr'}$ being projectors for our model

can be represented as

$$\hat{\rho}_{rr'} = \begin{pmatrix} \widehat{\chi^\dagger_{-\sigma_A}}(\vec{r})\,\widehat{\chi_{\sigma_A}}(\vec{r}) & \widehat{\chi^\dagger_{-\sigma_A}}(\vec{r})\,\widehat{\chi_{-\sigma_B}}(\vec{r}') \\ \widehat{\chi^\dagger_{\sigma_B}}(\vec{r}')\,\widehat{\chi_{\sigma_A}}(\vec{r}) & \widehat{\chi^\dagger_{\sigma_B}}(\vec{r}')\,\widehat{\chi_{-\sigma_B}}(\vec{r}') \end{pmatrix}$$

(3.3)

where $\left|\chi_{-\sigma_A}(\vec{r})\right|^2 = \langle 0|\,\widehat{\chi^\dagger_{-\sigma_A}}(\vec{r})\,\widehat{\chi_{\sigma_A}}(\vec{r})\,|0\rangle$ and $\left|\chi_{\sigma_B}(\vec{r}')\right|^2 = \langle 0|\,\widehat{\chi^\dagger_{\sigma_B}}(\vec{r}')\,\widehat{\chi_{-\sigma_B}}(\vec{r}')\,|0\rangle$ is the probability to find quasi-particle excitation on sublattice A and B respectively.

As is known [28, 29], secondary quantized Coulomb potential $\hat{V}(\vec{r}_i, \ \vec{r}_j)$ in valleys can be obtained by the action of the square of projector $\hat{\rho}_{rr'}$ (3.3) on two-point Coulomb potential $V(|\vec{r}_i - \vec{r}_j|)$:

$$\widehat{V}_{AB}(\vec{r}_i, \ \vec{r}_j) = \frac{1}{2}\widehat{\chi^\dagger_{-\sigma_A}}(\vec{r}_j)\,\widehat{\chi^\dagger_{-\sigma_A}}(\vec{r}_i)\,V(|\vec{r}_i - \vec{r}_j|)\widehat{\chi_{-\sigma_B}}(\vec{r}_i)\widehat{\chi_{-\sigma_B}}(\vec{r}_j),$$

$$\widehat{V}_{BA}(\vec{r}_i, \ \vec{r}_j) = \frac{1}{2}\widehat{\chi^\dagger_{\sigma_B}}(\vec{r}_j)\,\widehat{\chi^\dagger_{\sigma_B}}(\vec{r}_i)\,V(|\vec{r}_i - \vec{r}_j|)\widehat{\chi_{\sigma_A}}(\vec{r}_i)\widehat{\chi_{\sigma_A}}(\vec{r}_j).$$

(3.4)

The secondary quantize Coulomb interaction $\widehat{V}_{AB(BA)}(\vec{r}_i, \ \vec{r}_j)$ (3.4) in the Hartree–Fock approximation consists of the self-consistent potential $\hat{V}^{sc}$ and exchange interaction $\hat{\Sigma}^x$.

Let us find $\hat{V}^{sc}$ and $\hat{\Sigma}^x$ in graphene using the approach proposed in [30, 31].

3.2.   Wave function of the many-electron system

Let an arbitrary function ψ depends upon coordinates and spins of n electron: $\psi = \psi(\vec{r}_1, \vec{r}_2, \ldots, \vec{r}_n; s_1, \ldots s_n)$. To be a wave function of n electron system, the function $\psi(\vec{r}_{\alpha_1}, \vec{r}_{\alpha_2}, \ldots, \vec{r}_{\alpha_n})$ should satisfy the Pauli principle that is to be totally antisymmetric. Here index α_i, $i = 1, \ldots, n$ run over the set $\{1, 2, \ldots, n\}$ so that $\alpha_i \neq \alpha_j$ at $i \neq j$. This

can be done by representing this function as

$$\psi(\vec{r}_{\alpha_1}, \vec{r}_{\alpha_2}, \ldots, \vec{r}_{\alpha_n})$$
$$= \varepsilon(P_{\alpha_1\alpha_2\ldots\alpha_n})\,\psi(\vec{r}_1, \vec{r}_2, \ldots, \vec{r}_n)$$

(3.5)

where $P_{\alpha_1\alpha_2\ldots\alpha_n}$ is the permutation

$$P_{\alpha_1\alpha_2\ldots\alpha_n} = \begin{pmatrix} 1 & 2 & \ldots & n \\ \alpha_1 & \alpha_2 & \ldots & \alpha_n \end{pmatrix}.$$

(3.6)

Symbol $\varepsilon(P_{\alpha_1\alpha_2\ldots\alpha_n})$ designates a number equals $+1$, if the permutation $P_{\alpha_1\alpha_2\ldots\alpha_n}$ is even and equal to -1 if the permutation is odd one.

It is easy to prove that functions (3.5) satisfy the following equality

$$\sum_{\{\alpha_i\}_{i=1}^n} \psi(\vec{r}_{\alpha_1}, \vec{r}_{\alpha_2}, \ldots, \vec{r}_{\alpha_n}) = 0.$$

(3.7)

Let us split the left hand side of the expression (3.7) on functions one of which describe the spin configuration of the form $\{\uparrow\uparrow \ldots \uparrow\uparrow \mid \downarrow\downarrow\downarrow \ldots \downarrow\}$,

whereas another one –configurations $\{\uparrow\uparrow \ldots \uparrow\downarrow | \uparrow\downarrow\downarrow \ldots \downarrow\}$, $\{\uparrow\uparrow \ldots \uparrow\downarrow | \downarrow\uparrow\downarrow \ldots \downarrow\}$, $\{\uparrow\uparrow \ldots \uparrow\downarrow | \downarrow\downarrow\uparrow \ldots \downarrow\}$, ..., $\{\uparrow\uparrow \ldots \uparrow\downarrow | \downarrow\downarrow \ldots \downarrow\uparrow\}$ in the following way. To obtain the configuration $\{\uparrow\uparrow \ldots \uparrow\downarrow | \downarrow\downarrow \ldots \downarrow\uparrow\}$, electron from the set of k electrons with spin "up"is translated into the first position and permuted with all the rest

$n-1$ electrons. The configuration $\{\uparrow\uparrow \ldots \uparrow\downarrow | \downarrow\downarrow \ldots \uparrow\downarrow\}$ is obtained if an electron from the set of k electrons with spin "up"is translated to the first position and, excluding n−th electron, permute with $n - 2$ electrons. Doing in such a way and performing all possible permutation we arrive at

$$
\sum_{\{\alpha_i\}_{i=k+1}^n} \sum_{\{\alpha_i\}_{i=1}^k} \psi(\vec{r}_{\alpha_1}, \ldots, \vec{r}_{\alpha_{k-1}}, \vec{r}_{\alpha_k} | \vec{r}_{\alpha_{k+1}}, \vec{r}_{\alpha_{k+2}}, \ldots, \vec{r}_{\alpha_n})
$$
$$
= \sum_{\{\alpha_i\}_{i=k+1}^n} \sum_{\{\alpha_i\}_{i=1}^k} (\psi(\vec{r}_{\alpha_1}, \ldots, \vec{r}_{\alpha_{k-1}}, \vec{r}_{\alpha_{k+1}} | \vec{r}_{\alpha_k}, \vec{r}_{\alpha_{k+2}}, \ldots, \vec{r}_{\alpha_n}) + \ldots
$$
$$
+ \psi(\vec{r}_{\alpha_1}, \ldots, \vec{r}_{\alpha_{k-1}}, \vec{r}_{\alpha_{k+l}} | \vec{r}_{\alpha_{k+1}}, \ldots, \vec{r}_{\alpha_{k+l-1}}, \vec{r}_{\alpha_k}, \vec{r}_{\alpha_{k+l+1}}, \ldots, \vec{r}_{\alpha_n}) + \ldots
$$
$$
+ \psi(\vec{r}_{\alpha_1}, \ldots, \vec{r}_{\alpha_{k-1}}, \vec{r}_{\alpha_n} | \vec{r}_{\alpha_{k+1}}, \ldots, \vec{r}_{\alpha_{k-n}}, \vec{r}_{\alpha_k})).
$$

(3.8)

From the expression (3.8) it follows the identity

$$
\psi(\vec{r}_1, \ldots, \vec{r}_{k-1}, \vec{r}_k | \vec{r}_{k+1}, \vec{r}_{k+2}, \ldots, \vec{r}_n) = \psi(\vec{r}_1, \ldots, \vec{r}_{k-1}, \vec{r}_{k+1} | \vec{r}_k, \vec{r}_{k+2}, \ldots, \vec{r}_n)
$$
$$
+ \ldots + \psi(\vec{r}_1, \ldots, \vec{r}_{k-1}, \vec{r}_{k+l} | \vec{r}_{k+1}, \ldots, \vec{r}_{k+l-1}, \vec{r}_k, \vec{r}_{k+l+1}, \ldots, \vec{r}_n)
$$
$$
+ \ldots + \psi(\vec{r}_1, \ldots, \vec{r}_{k-1}, \vec{r}_n | \vec{r}_{k+1}, \ldots, \vec{r}_{k-n}, \vec{r}_k).
$$

(3.9)

In a graphic form the partition (3.9) demonstrates in Fig. 2.

The wave function on the right hand side of symbolic expression in Fig. 2 describes the configuration obtained by cyclic permutation of the electron configuration shown on the left side in Fig. 2.

Electron function is symmetric under cyclic permutations, and mathematical notation for this property of cyclic symmetry is the expression (3.9). The set of functions (3.5) is a basis set for construction of a wave function for many-electron system. Slater determinants possess the properties of the introduced basis set.

3.3. Hole formalism

We use the hole formalism, choosing as the vacuum state the non-degenerate ground state of an atom in the absence of interaction of electrons as quasiparticles. Single-particle state

representing itself an appearance of a vacancy in the filled electron shell is called a hole quasi-particle excitation.

In representation of secondary quantization, single-particle states are given by creation operators $\widehat{\psi}^\dagger(x_i^L)$ and annihilation operators $\widehat{\psi}(x_i^L)$ of i-th particle on a sublattice L with generalized coordinates $x_i^L = \{\vec{r}_i, t_i, \sigma_i^L\}$, being a radius-vector $\vec{r}_i$, time t_i and spin projection σ_i^L.

These operators satisfy the commutation relations

$$
\widehat{\psi}(x^{L'}) \, \widehat{\psi^\dagger}(x^L) + \widehat{\psi^\dagger}(x^L) \, \widehat{\psi}(x^{L'})
$$
$$
= \delta(x^L - x^{L'}), \quad (3.10)
$$

$$
\widehat{\psi}(x^{L'}) \, \widehat{\psi}(x^L) + \widehat{\psi}(x^L) \, \widehat{\psi}(x^{L'}) = 0. \quad (3.11)
$$

Now one can introduce the creation operator of a hole. Since the wave function can be written as

$$\{\underbrace{\uparrow\uparrow\uparrow\uparrow}_{k} | \underbrace{\downarrow\downarrow\downarrow\downarrow}_{n-k}\} = \{\underbrace{\uparrow\uparrow\uparrow\downarrow}_{k} | \underbrace{\uparrow\downarrow\downarrow\downarrow}_{n-k}\} + \{\underbrace{\uparrow\uparrow\uparrow\downarrow}_{k} | \underbrace{\downarrow\uparrow\downarrow\downarrow}_{n-k}\} + \{\underbrace{\uparrow\uparrow\uparrow\downarrow}_{k} | \underbrace{\downarrow\downarrow\uparrow\downarrow}_{n-k}\} + \ldots + \{\underbrace{\uparrow\uparrow\uparrow\downarrow}_{k} | \underbrace{\downarrow\downarrow\downarrow\uparrow}_{n-k}\}$$

FIG. 2: Graphical representation of the cyclic symmetry property of electron wave function.

$$\widehat{\psi^\dagger}_{(n-k)\downarrow}(\vec{r}_n, \ldots, \vec{r}_{k+2}, \vec{r}_{k+1}) \, \widehat{\psi^\dagger}_{k\uparrow}(\vec{r}_k, \vec{r}_{k-1}, \ldots, \vec{r}_1)|0> = \left[\widehat{\psi}_{n\downarrow}(\vec{r}_n)\right.$$

$$+\widehat{\psi}_{(n+1)\uparrow}(\vec{r}_{n+1})\Big] \, \widehat{\psi^\dagger}_{(n-k+1)\downarrow}(\vec{r}_{n+1}, \ldots, \vec{r}_{k+2}, \vec{r}_{k+1}) \, \widehat{\psi^\dagger}_{k\uparrow}(\vec{r}_k, \vec{r}_{k-1}, \ldots, \vec{r}_1)|0> \qquad (3.12)$$

$$= \left[\widehat{\psi}_{n\downarrow}(\vec{r}_n) + \widehat{\psi}_{(n+1)\uparrow}(\vec{r}_{n+1})\right] \, |\psi_1, \ldots, \psi_{n+1} >,$$

then the operator $\left[\widehat{\psi}_{n\downarrow}(\vec{r}_n) + \widehat{\psi}_{(n+1)\uparrow}(\vec{r}_{n+1})\right]$ is the hole creation operator at the position of an electron paired with an external n-th electron.

Here the secondary quantized wave function of the system

$$\widehat{\psi^\dagger}_{(n-k)\downarrow}(\vec{r}_n, \ldots, \vec{r}_{k+2}, \vec{r}_{k+1}) \, \widehat{\psi^\dagger}_{k\uparrow}(\vec{r}_k, \vec{r}_{k-1}, \ldots, \vec{r}_1)$$

describes the configuration of k electrons with spin "up" , $n - k$ electrons with spin "down" wherein $n = 2k + 1$; that is there exist one valent electron $|0 >$ is the vacuum state. The wave function (3.12) describes the system with an unpaired external electron and a hole at a

place of the electron, paired with an external n-th electron. Let in time moment t valley polarization occurs. Then at the same time moment t the secondary quantized wave function of the system can be obtained as a result of cyclic permutation $P^{(cycl)}(t)$:

$$P^{(cycl)}(t) \left[\widehat{\psi}_{n\downarrow}(\vec{r}_n) + \widehat{\psi}_{(n+1)\uparrow}(\vec{r}_{n+1})\right] |\psi_1, \ldots, \psi_{n+1} > . \qquad (3.13)$$

Due to the fact that operators $P^{(cycl)}(t)$ and $\left[\widehat{\psi}_{n\downarrow}(\vec{r}_n) + \widehat{\psi}_{(n+1)\uparrow}(\vec{r}_{n+1})\right]$ commutes each other, and account for the permutation operator

definition shown graphically in Fig. 2 the expression (3.13) can be rewritten in the form

$$P^{(cycl)}(t) \left[\widehat{\psi}_{n\downarrow}(\vec{r}_n) + \widehat{\psi}_{(n+1)\uparrow}(\vec{r}_{n+1}) \right] |\psi_1, \ldots, \psi_{n+1} >$$

$$= \left[\widehat{\psi}_{n\downarrow}(\vec{r}_n) + \widehat{\psi}_{(n+1)\uparrow}(\vec{r}_{n+1}) \right] P^{(cycl)}(t)|\psi_1, \ldots, \psi_{n+1} >$$

$$= \left[\sum_{m=1}^{k} c_{nm}(t)\, \widehat{\psi}_{m\downarrow}(\vec{r}_m,\, t) + \sum_{m=k+1}^{n} c_{nm}(t)\, \widehat{\psi}_{(m+1)\uparrow}(\vec{r}_{m+1},\, t) \right] \qquad (3.14)$$

$$\times\, P_m^{(cycl)}|\psi_1,\, \ldots,\, \psi_{n+1} > \;=\; \sum_{m=1}^{n} c_{nm}(t)\, \widehat{\psi}(x_m^L)\, P_m^{(cycl)}|\psi_1,\, \ldots,\, \psi_{n+1} >$$

where m-th term in the sum describes a hole (vacancy) at a place of m-th valley electron creating after a cyclic permutation $P_m^{(cycl)}$ in the sense of (3.9), matrix $\|c_{nm}(t)\|$ transfers the hole creation operator at place of n-th electron into operator of hole creation at place of m-th electron of valley L.

According to the properties of cyclic symmetry (3.9), one can formally write the expression

$$\left[\widehat{\psi}_{n\downarrow}(\vec{r}_n) + \widehat{\psi}_{(n+1)\uparrow}(\vec{r}_{n+1}) \right] = \sum_{m=1}^{n} c_{nm}(t)\, \widehat{\psi}(x_m^L)\, P_m^{(cycl)}. \qquad (3.15)$$

From this it follows that $\sum_{m=1}^{n} c_{nm}(t)\,\widehat{\psi}(x_m^L)$ must obey the same quantum equations of motion as $\left[\widehat{\psi}_{n\downarrow}(\vec{r}_n) + \widehat{\psi}_{(n+1)\uparrow}(\vec{r}_{n+1}) \right]$. Heisenberg equation of motion for a hole creation operator $\left[\widehat{\psi}_{n\downarrow}(\vec{r}_n) + \widehat{\psi}_{(n+1)\uparrow}(\vec{r}_{n+1}) \right]$ has the form

$$\frac{\hbar}{i} \frac{\partial}{\partial t} \left[\widehat{\psi}_{n\downarrow}(\vec{r}_n) + \widehat{\psi}_{(n+1)\uparrow}(\vec{r}_{n+1}) \right] = \left[\left[\widehat{\psi}_{n\downarrow}(\vec{r}_n) + \widehat{\psi}_{(n+1)\uparrow}(\vec{r}_{n+1}) \right],\ \widehat{\mathcal{H}} \right], \qquad (3.16)$$

$$\widehat{\mathcal{H}} = \left(\sum_{i=1}^{n} \int \widehat{H}(x_i)\, d\vec{r}_i \;+\; \sum_{i>j=1}^{n} \iint \widehat{V}(x_i, x_j)\, d\vec{r}_i\, d\vec{r}_j \right), \qquad (3.17)$$

$$\widehat{H}(x_i) = \widehat{\psi^{\dagger}}(x_i^L)\, H(\vec{r}_i)\, \widehat{\psi}(x_i^L); \quad \widehat{V}(x_i, x_j) = \frac{1}{2}\widehat{\psi^{\dagger}}(x_j^L)\, \widehat{\psi^{\dagger}}(x_i^L)\, V(\vec{r}_i - \vec{r}_j)\, \widehat{\psi}(x_i^{L'})\, \widehat{\psi}(x_j^{L'}) \qquad (3.18)$$

where $[\,\cdot\,,\,\cdot\,]$ is the commutator of operators, $\widehat{\mathcal{H}}$ is the Hamilton operator obtained from operators (3.1) by the procedure of secondary quantization (3.4).

Substituting the expression (3.15) into equation of motion (3.16), we find the equation of motion for hole creation operator $\sum_{m=1}^{n} c_{nm}(t)\, \widehat{\psi}(x_m^L)$ at place of m-th electron of valley L:

$$\frac{\hbar}{i}\frac{\partial}{\partial t}\sum_{m=1}^{n} c_{nm}(t)\widehat{\psi}(x_m^L)P_m^{(cycl)} = \sum_{m,i=1}^{n} c_{nm}(t)\int d\vec{r}_i \left\{\widehat{\psi}(x_m^L)\right.$$

$$\times \left[\widehat{\psi^\dagger}(x_i^L)\,H(\vec{r}_i)\,\widehat{\psi}(x_i^L) + \sum_{j=1}^{n}\int\frac{d\vec{r}_j}{2}\widehat{\psi^\dagger}(x_j^L)\,\widehat{\psi^\dagger}(x_i^L)\,V(\vec{r}_i-\vec{r}_j)\,\widehat{\psi}(x_i^{L'})\,\widehat{\psi}(x_j^{L'})\right]$$

$$-\left[\widehat{\psi^\dagger}(x_i^L)\,H(\vec{r}_i)\,\widehat{\psi}(x_i^L) + \sum_{j=1}^{n}\int\frac{d\vec{r}_j}{2}\,\widehat{\psi^\dagger}(x_j^L)\,\widehat{\psi^\dagger}(x_i^L)\,V(\vec{r}_i-\vec{r}_j)\widehat{\psi}(x_i^{L'})\widehat{\psi}(x_j^{L'})\right]\widehat{\psi}(x_m^L)\right\}\,P_m^{(cycl)}\,.$$

$$(3.19)$$

Here $j < i$. Using the permutation rules (3.10), (3.11) of quantized fermionic fields and relation $\langle 0|\widehat{\psi^\dagger} = 0$, we transform the equation (3.19) to the form

$$\frac{\hbar}{i}\frac{\partial}{\partial t}\sum_{m=1}^{n} c_{nm}(t)\,\widehat{\psi}(x_m^L)\,P_m^{(cycl)} = \sum_{m,i=1}^{n} c_{nm}(t)\int d\vec{r}_i \left\{[\delta(x_i^L-x_m^L)\right.$$

$$\times H(\vec{r}_i)\,\widehat{\psi}(x_i) + \sum_{j=1}^{n}\int\frac{d\vec{r}_j}{2}\,\delta(x_j^L-x_m^L)\,\widehat{\psi^\dagger}(x_i^L)\,V(\vec{r}_i-\vec{r}_j)\,\widehat{\psi}(x_i^{L'})\,\widehat{\psi}(x_j^{L'})\right] \qquad (3.20)$$

$$-\left[\sum_{j=1}^{n}\int d\vec{r}_j\frac{\delta(x_i^L-x_m^L)}{2}\,\widehat{\psi^\dagger}(x_j^L)\,V(\vec{r}_i-\vec{r}_j)\,\widehat{\psi}(x_i^{L'})\,\widehat{\psi}(x_j^{L'})\right]\right\}\,P_m^{(cycl)},\;\; \text{for } j < i$$

where $\delta(x_k^L-x_m^L)$ is the Dirac δ-function. Taking a time derivative in the left hand side and after integration with δ-function in right hand side of equation (3.20), finally we obtain

$$\left(\frac{\hbar}{i}\frac{\partial\ln c_{nm}(t)}{\partial t} - \widehat{\varepsilon}\,\widehat{I}\right)\,\widehat{\psi}(x_m^L)\,P_m^{(cycl)} = \left(H(\vec{r}_m)\widehat{\psi}(x_m^L) + \frac{1}{2}\sum_{i=1}^{n}\int d\vec{r}_i\,\left(\widehat{\psi^\dagger}(x_i^L)\right.\right.$$

$$\times V(\vec{r}_i-\vec{r}_m)\,\widehat{\psi}(x_i^{L'})\,\widehat{\psi}(x_m^{L'}) - \widehat{\psi^\dagger}(x_i^L)\,V(\vec{r}_m-\vec{r}_i)\,\widehat{\psi}(x_m^{L'})\,\widehat{\psi}(x_i^{L'})\big)\big)\,P_m^{(cycl)} \qquad (3.21)$$

$$= \left(H(\vec{r}_m)\,\widehat{\psi}(x_m^L) - \sum_{i=1}^{n}\int d\vec{r}_i\,\widehat{\psi^\dagger}(x_i^L)\,V(\vec{r}_i-\vec{r}_m)\,\widehat{\psi}(x_m^{L'})\,\widehat{\psi}(x_i^{L'})\right)\,P_m^{(cycl)}$$

where $\widehat{I}$ is the identity operator, $\widehat{\varepsilon}$ is the hole energy operator since

$$\widehat{\psi}(x_m^L) = \widehat{\psi}(\vec{r}_m, \ \sigma_m^L) \exp(-i\widehat{\varepsilon}\,\widehat{I}t/\hbar).$$

Right hand side of the equation (3.21) is rewritten accounting for matrix multiplication rules. Now we can find the equations describing a single-particle state when neglecting correlations in

motion of electrons in respect to each other. For considered configuration shown in Fig. 2 we assume that all electrons with spin "up" move independently in respect to electrons with spin "down". In other words, their motion is uncorrelated. Therefore the wave function of such configuration is factorized as follows:

$$\widehat{\psi^{\dagger}}_{(n-k)\downarrow}(\vec{r}_n, \ \ldots, \ \vec{r}_{k+2}, \ \vec{r}_{k+1}) \ \widehat{\psi^{\dagger}}_{k\uparrow}(\vec{r}_k, \ \vec{r}_{k-1}, \ \ldots, \ \vec{r}_1) \ |0> = \ |\psi_1, \ldots, \psi_n >$$

$$= \ |\psi_n, \ \ldots, \ \psi_{k+2}, \ \psi_{k+1} > \ |\psi_k, \ \psi_{k-1}, \ \ldots, \ \psi_1 > \tag{3.22}$$

$$= \ \widehat{\psi^{\dagger}}_{(n-k)\downarrow}(\vec{r}_n, \ \ldots, \ \vec{r}_{k+2}, \ \vec{r}_{k+1}) \ |0\downarrow> \ \widehat{\psi^{\dagger}}_{k\uparrow}(\vec{r}_k, \ \vec{r}_{k-1}, \ \ldots, \ \vec{r}_1) \ |0\uparrow> .$$

From this, the expansion for the vacuum state $|0>$ follows:

$$|0\rangle \ = \ |0\downarrow\rangle \ |0\uparrow\rangle \ \equiv \ |0, \ \sigma_m\rangle \ |0, \ -\sigma_i\rangle \ , \tag{3.23}$$

which means that the vacuum state $|0\rangle$ consists of

vacuum states of spin "up" $|0\downarrow\rangle$ and spin "down" $|0\uparrow\rangle$.

Hermitian conjugation of the equation (3.21) reads

$$\left(i\hbar\frac{\partial \ln c_{nm}(t)}{\partial t} - \widehat{\varepsilon}^{\dagger}\widehat{I}\right) P_m^{(cycl)} \widehat{\psi^{\dagger}}(x_m^L) \ = \ P_m^{(cycl)} \left(H(\vec{r}_m) \ \widehat{\psi^{\dagger}}(x_m^L)\right.$$

$$-\sum_{i=1}^{n} \int d\vec{r}_i \ \widehat{\psi^{\dagger}}(x_i^{L'}) V(\vec{r}_i - \vec{r}_m) \widehat{\psi^{\dagger}}(x_m^{L'}) \ \widehat{\psi}(x_i)\bigg) = P_m^{(cycl)} \left(H(\vec{r}_m)\right. \tag{3.24}$$

$$\times \ \widehat{\psi^{\dagger}}(x_m^L) - \sum_{i=1}^{n} \int d\vec{r}_i \ \widehat{\psi^{\dagger}}(x_m^{L'}) \ V(\vec{r}_i - \vec{r}_m) \ \widehat{\psi^{\dagger}}(x_i^{L'}) \ \widehat{\psi}(x_i^L)\bigg) .$$

Acting by the Hermitian conjugated equation (3.24) on the vacuum state (3.23) we find

$$\left(i\hbar\frac{\partial \ln c_{nm}(t)}{\partial t} - \widehat{\varepsilon}^{\dagger}\widehat{I}\right) P_m^{(cycl)} \widehat{\psi^{\dagger}}_{\sigma_m^L}(\vec{r}_m)|0, \ \sigma_m> \ |0, \ -\sigma_i>$$

$$= P_m^{(cycl)} \left(H(\vec{r}_m) \ \widehat{\psi^{\dagger}}_{\sigma_m^L}(\vec{r}_m) - \sum_{i=1}^{n} \ \int d\vec{r}_i\right. \tag{3.25}$$

$$\times \ \widehat{\psi^{\dagger}}_{\sigma_m^{L'}}(\vec{r}_m) \ \widehat{\psi^{\dagger}}_{\sigma_i^{L'}}(\vec{r}_i) \ V(\vec{r}_i - \vec{r}_m) \ \widehat{\psi}_{-\sigma_i^L}(\vec{r}_i)\bigg) |0, \ \sigma_m> \ |0, \ -\sigma_i> .$$

Permutation $P_m^{(cycl)}$ (3.9), entering equation (3.25), is expressed as (permuting separately symbols $L(L')$

and $\pm\sigma_k$):

$$P_m^{(cycl)} \, \widehat{\psi^\dagger}_{\sigma_m^{L'}}(\vec{r}_m) \, \widehat{\psi^\dagger}_{\sigma_i^{L'}}(\vec{r}_i) \, \widehat{\psi}_{-\sigma_i^L}(\vec{r}_i)$$
$$= \widehat{\psi^\dagger}_{-\sigma_i^{L'}}(\vec{r}_m) \, \widehat{\psi^\dagger}_{\sigma_i^L}(\vec{r}_i) \, \widehat{\psi}_{\sigma_m^{L'}}(\vec{r}_i) - \widehat{\psi^\dagger}_{\sigma_m^L}(\vec{r}_m) \, \widehat{\psi^\dagger}_{-\sigma_i^{L'}}(\vec{r}_i) \, \widehat{\psi}_{\sigma_i^{L'}}(\vec{r}_i). \tag{3.26}$$

Substitution of the explicit expression for $P_m^{(cycl)}$ (3.26) into (3.25) gives the equation

$$\left(i\hbar \frac{\partial \ln c_{nm}(t)}{\partial t} - \widehat{\varepsilon}^\dagger \widehat{I} \right) \widehat{\psi^\dagger}_{\sigma_m^L}(\vec{r}_m) \, |0, \, \sigma_m\rangle \, |0, \, -\sigma_i\rangle \;\; = \;\; \left[H(\vec{r}_m) \, \widehat{\psi^\dagger}_{\sigma_m^L}(\vec{r}_m) \right.$$
$$- \sum_{i=1}^{n} \int d\vec{r}_i \, \left(\widehat{\psi^\dagger}_{-\sigma_i^{L'}}(\vec{r}_m) \, V(\vec{r}_i - \vec{r}_m) \, \widehat{\psi^\dagger}_{\sigma_i^L}(\vec{r}_i) \, \widehat{\psi}_{\sigma_m^{L'}}(\vec{r}_i) \; - \; \widehat{\psi^\dagger}_{\sigma_m^L}(\vec{r}_m) \, V(\vec{r}_i - \vec{r}_m) \right.$$
$$\left. \left. \times \, \widehat{\psi^\dagger}_{-\sigma_i^{L'}}(\vec{r}_i) \, \widehat{\psi}_{\sigma_i^{L'}}(\vec{r}_i) \right) \right] \, |0, \, \sigma_m\rangle \, |0, \, -\sigma_i\rangle. \tag{3.27}$$

Multiplying equation (3.27) from the left on the vector $\langle 0, \, \sigma_i|$, we get

$$i\hbar \frac{\partial \ln c_{nm}(t)}{\partial t} \, \widehat{\psi^\dagger}_{\sigma_m^L}(\vec{r}_m) \, |0, \, \sigma_m\rangle \; - \; \langle 0, \, \sigma_i| \, \widehat{\varepsilon}^\dagger \widehat{I} \, |0, \, -\sigma_i\rangle \, \widehat{\psi^\dagger}_{\sigma_m^L}(\vec{r}_m) \, |0, \, \sigma_m\rangle$$
$$= H(\vec{r}_m) \, \widehat{\psi^\dagger}_{\sigma_m^L}(\vec{r}_m) \, |0, \, \sigma_m\rangle$$
$$- \sum_{i=1}^{n} \int d\vec{r}_i \, \widehat{\psi^\dagger}_{-\sigma_i^{L'}}(\vec{r}_m) \, |0, \, \sigma_m\rangle \, V(\vec{r}_i - \vec{r}_m) \, \langle 0, \, \sigma_i| \, \widehat{\psi^\dagger}_{\sigma_i^L}(\vec{r}_i) \, \widehat{\psi}_{\sigma_m^{L'}}(\vec{r}_i) \, |0, \, -\sigma_i\rangle$$
$$+ \sum_{i=1}^{n} \int d\vec{r}_i \, \widehat{\psi^\dagger}_{\sigma_m^L}(\vec{r}_m) \, |0, \, \sigma_m\rangle \, V(\vec{r}_i - \vec{r}_m) \, \langle 0, \, \sigma_i| \, \widehat{\psi^\dagger}_{-\sigma_i^{L'}}(\vec{r}_i) \, \widehat{\psi}_{\sigma_i^{L'}}(\vec{r}_i) \, |0, \, -\sigma_i\rangle \,, \tag{3.28}$$

accounting for that $< 0, \, \sigma_i | 0, \, -\sigma_i >= 1$. If one introduces the designation $\widehat{\psi^\dagger}_{\sigma_j}(\vec{r}_k) \, |0, \, \sigma_j\rangle \equiv \psi_j(x_k)$, and represent the identity operator in the form of expansion

$$\widehat{I} = \sum_{j=1}^{n} \widehat{\psi^\dagger}_{\sigma_j}(\vec{r}_k) \, |0, \, \sigma_j\rangle\langle 0, \, \sigma_j| \, \widehat{\psi}_{\sigma_j}(\vec{r}_k) \equiv \sum_{j=1}^{n} P_j,$$

then the equation (3.28) can be rewritten as

$$i\hbar \frac{\partial \ln c_{nm}(t)}{\partial t} \, \psi_m(x_m^L) - \sum_{j=1}^{n} \widehat{\varepsilon}^\dagger P_j \, \psi_m(x_m^L) = H(\vec{r}_m) \, \psi_m(x_m^L) + \sum_{i=1}^{n} \int d\vec{r}_i$$
$$\times \, \left(\psi_m(x_m^L) \, V(\vec{r}_i - \vec{r}_m) \, \psi_i^*(\bar{x}_i^{L'}) \, \psi_i^*(x_i^{L'}) \; - \; \psi_i(\bar{x}_m^{L'}) \, V(\vec{r}_i - \vec{r}_m) \, \psi_i^*(x_i^L) \, \psi_m^*(x_m^{L'}) \right). \tag{3.29}$$

Here $\bar{x}_k^{L'} = \{\vec{r}_k, \, t_k, \, -\sigma_k^{L'}\}$. The equation (3.29), taken in initial moment of time $t = 0$, describes

single-particle state $\psi_m(x_m^L)$:

$$\left[H(\vec{r}_m) + \widehat{V}^{sc}(x_m) + \widehat{\Sigma}^x(x_m) \right] \psi_m(x_m^L)$$
$$= \left(\varepsilon_m(0) - \sum_{j=1}^{n} \widehat{\varepsilon}^\dagger P_j \right) \psi_m(x_m^L) \tag{3.30}$$

where the time derivative taken in initial moment of time $t = 0$ is designated as ε_m:

$$\varepsilon_m(0) = i\hbar \frac{\partial \ln c_{nm}(t)}{\partial t}\Bigg|_{t=0},$$

$\widehat{V}^{sc}$ и $\widehat{\Sigma}x$ are operators of Coulomb and exchange interactions:

$$\widehat{V}^{sc}(x_m)\psi_m(x_m^L) = \sum_{i=1}^{n} \int d\vec{r}_i \psi_m(x_m^L)\, V(\vec{r}_i - \vec{r}_m)\, \psi_i^*(\bar{x}_i^{L'})\, \psi_i^*(x_i^{L'}), \qquad (3.31)$$

$$\widehat{\Sigma}^x(x_i)\psi_n(x_i) = -\sum_{i=1}^{n} \int d\vec{r}_i \psi_i(\bar{x}_m^{L'})\, V(\vec{r}_i - \vec{r}_m)\psi_i^*(x_i^L)\, \psi_m^*(x_m^{L'}). \qquad (3.32)$$

Since operators $\widehat{V}^{sc}$ and $\widehat{\Sigma}^x$ enter into the expression (3.30) with opposite signs, self-action terms are mutually eliminated.

Now we suppose that there exist a representation where the hole energy operator $\hat{\varepsilon}^\dagger$ in equation (3.30) is diagonalized $\hat{\varepsilon}^\dagger = \varepsilon(k_i)I$.

Accounting of this diagonalization condition and replacement $\vec{r}_m \to \vec{r}_i$ in equation (3.30) allows us to describe the polarization of valleys as quasi-particle excitation with the energy $\varepsilon(k_i)$, and the steady state given by the solution of the eigenproblem

$$\left[H(\vec{r}_i) + \widehat{V}^{sc}(k_i x_i) - \widehat{\Sigma}^x(k_i x_i) \right] \psi_m(k_i x_i^L) = \left(\varepsilon_m(0) - \sum_{j=1}^{n} \hat{\varepsilon}^\dagger P_j \right) \psi_m(k_i x_i^L), \qquad (3.33)$$

$$\hat{\varepsilon}^\dagger = \varepsilon(k_i)I. \qquad (3.34)$$

Now, using (3.4) and (3.29, 3.31, 3.32) we can write the final expression for relativistic exchange Σ_{rel}^x and self-consistent Coulomb potential V_{rel}^{sc} :

$$\Sigma_{rel}^x \begin{pmatrix} \widehat{\chi}_{-\sigma_A}^\dagger(\vec{r}) \\ \widehat{\chi}_{\sigma_B}^\dagger(\vec{r}) \end{pmatrix} |0, -\sigma\rangle\, |0, \sigma\rangle = \begin{pmatrix} 0 & (\Sigma_{rel}^x)_{AB} \\ (\Sigma_{rel}^x)_{BA} & 0 \end{pmatrix} \begin{pmatrix} \widehat{\chi}_{-\sigma_A}^\dagger(\vec{r}) \\ \widehat{\chi}_{\sigma_B}^\dagger(\vec{r}) \end{pmatrix} |0, -\sigma\rangle\, |0, \sigma\rangle, \qquad (3.35)$$

$$(\Sigma_{rel}^x)_{AB}\, \widehat{\chi}_{\sigma_B}^\dagger(\vec{r})\, |0, \sigma\rangle$$

$$= -\sum_{i=1}^{N_v N} \int d\vec{r}_i \widehat{\chi}_{\sigma_{i_B}}^\dagger(\vec{r})\, |0, \sigma\rangle\, \langle 0, -\sigma_i | \widehat{\chi}_{-\sigma_{i_A}}^\dagger(\vec{r}_i) V(\vec{r}_i - \vec{r}) \widehat{\chi}_{-\sigma_B}(\vec{r}_i)|0, -\sigma_{i'}\rangle, \qquad (3.36)$$

$$(\Sigma_{rel}^x)_{BA}\, \widehat{\chi}_{-\sigma_A}^\dagger(\vec{r})\, |0, -\sigma\rangle$$

$$= -\sum_{i'=1}^{N_v N} \int d\vec{r}_{i'} \widehat{\chi}_{-\sigma_{i'}^A}^\dagger(\vec{r})\, |0, -\sigma\rangle\, \langle 0, \sigma_{i'} | \widehat{\chi}_{\sigma_{i'}^B}^\dagger(\vec{r}_{i'}) V(\vec{r}_{i'} - \vec{r}) \widehat{\chi}_{\sigma_A}(\vec{r}_{i'})|0, \sigma_i\rangle; \qquad (3.37)$$

$$V_{rel}^{sc} \begin{pmatrix} \widehat{\chi_{-\sigma_A}^{\dagger}}(\vec{r}) \\ \widehat{\chi_{\sigma_B}^{\dagger}}(\vec{r}) \end{pmatrix} |0,-\sigma\rangle |0,\sigma\rangle = \begin{pmatrix} (V_{rel}^{sc})_{AA} & 0 \\ 0 & (V_{rel}^{sc})_{BB} \end{pmatrix} \begin{pmatrix} \widehat{\chi_{-\sigma_A}^{\dagger}}(\vec{r}) \\ \widehat{\chi_{\sigma_B}^{\dagger}}(\vec{r}) \end{pmatrix} |0,-\sigma\rangle |0,\sigma\rangle, \quad (3.38)$$

$$(V_{rel}^{sc})_{AA} = \sum_{i=1}^{N_v N} \int d\vec{r}_i \langle 0,-\sigma_i | \widehat{\chi}_{-\sigma_i^A}^{\dagger}(\vec{r}_i) V(\vec{r}_i - \vec{r}) \widehat{\chi}_{\sigma_i^A}(\vec{r}_i) |0,-\sigma_i\rangle, \quad (3.39)$$

$$(V_{rel}^{sc})_{BB} = \sum_{i'=1}^{N_v N} \int d\vec{r}_{i'} \langle 0,\sigma_{i'} | \widehat{\chi}_{\sigma_{i'}^B}^{\dagger}(\vec{r}_{i'}) V(\vec{r}_{i'} - \vec{r}) \widehat{\chi}_{-\sigma_{i'}^B}(\vec{r}_{i'}) |0,\sigma_{i'}\rangle; \quad (3.40)$$

4. The band structure of monolayer graphene in approximation of the Dirac–Hartree–Fock self-consistent field

In papers [19, 24–27] we proposed two-dimensional approximation of exchange interactions and quasi-relativistic approximation of Dirac–Hartree–Fock self-consistent field with additional assumption on spin ordering of sublattices A, B in graphene. In such an approach, two-dimensional graphene is described by the following steady state equation, e.g., for the secondary quantized fermionic field $\widehat{\chi}_{+\sigma_B}^{\dagger}$:

$$\left[c\vec{\sigma}_{2D}^{BA} \cdot \widehat{\vec{p}}_{AB} - \widetilde{\Sigma_{AB}\Sigma_{BA}}(\vec{p}_{AB}) \right] \widehat{\widetilde{\chi}}_{+\sigma_B}^{\dagger}(\vec{r}) |0,\sigma\rangle = cE_{qu}(p_{AB}) \widehat{\widetilde{\chi}}_{+\sigma_B}^{\dagger}(\vec{r}) |0,\sigma\rangle \quad (4.1)$$

where $\widetilde{\Sigma_{AB}\Sigma_{BA}} = -(\Sigma_{rel}^x)_{BA} (\Sigma_{rel}^x)_{AB}$, $\widehat{\widetilde{\chi}}_{+\sigma_B}^{\dagger}(\vec{r})|0,\sigma\rangle = (\Sigma_{rel}^x)_{AB} \widehat{\chi}_{+\sigma_B}^{\dagger}(\vec{r})|0,\sigma\rangle$, $\vec{\sigma}_{2D}^{AB} = (\Sigma_{rel}^x)_{BA} \vec{\sigma}_{2D} (\Sigma_{rel}^x)_{BA}^{-1}$, $\vec{\sigma}_{2D}$ is the $2D$-vector of Pauli matrixes,

$$\widehat{\vec{p}}_{AB} = (\Sigma_{rel}^x)_{BA} \widehat{\vec{p}} (\Sigma_{rel}^x)_{BA}^{-1},$$

$\widehat{\vec{p}}$ is the momentum operator, transformation 2D matrices $(\Sigma_{rel}^x)_{BA}$, $(\Sigma_{rel}^x)_{AB}$ are determined by an exchange interaction term Σ_{rel}^x (3.35, 3.36, 3.37), $\vec{p}_{AB}$ is an eigenvalue of the operator $\widehat{\vec{p}}_{AB}$: $\vec{p}_{AB} = \langle \widetilde{\chi} | \widehat{\vec{p}}_{AB} | \widetilde{\chi} \rangle$.

In Figs. 3, 4 it is shown as the unit circumference $\vec{p}$: $|\vec{p}| = 1$ is transformed under the action of exchange operators:

$$(\Sigma_{rel}^x)_{AB} \ \vec{p} (\Sigma_{rel}^x)_{AB}^{-1}, \quad (4.2)$$

$$(\Sigma_{rel}^x)_{BA} (\Sigma_{rel}^x)_{AB} \ \vec{p} (\Sigma_{rel}^x)_{AB}^{-1} (\Sigma_{rel}^x)_{BA}^{-1} \quad (4.3)$$

$$(\Sigma_{rel}^x)_{AB} (\Sigma_{rel}^x)_{BA} (\Sigma_{rel}^x)_{AB} \ \vec{p} (\Sigma_{rel}^x)_{AB}^{-1} (\Sigma_{rel}^x)_{BA}^{-1} (\Sigma_{rel}^x)_{AB}^{-1}. \quad (4.4)$$

Transformations (4.2) and $(\Sigma_{rel}^x)_{BA} \ \vec{p} \ (\Sigma_{rel}^x)_{BA}^{-1}$ deform the circumference into extremely elongated ellipses rotated on angle 90° in respect to each other (see Fig. 3).

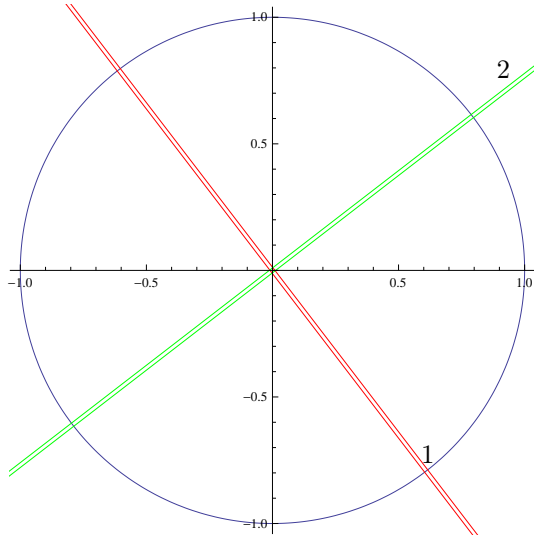As one can see from Fig. 4, the transformation (4.3) of already highly stretched

FIG. 3. Transformations of circumference $\vec{p} : |\vec{p}| = 1$ in momentum space into ellipses under the action of exchange operators: $(\Sigma^x_{rel})_{AB} \; \vec{p} \; (\Sigma^x_{rel})^{-1}_{AB}$ (1) and $(\Sigma^x_{rel})_{BA} \; \vec{p} \; (\Sigma^x_{rel})^{-1}_{BA}$ (2) respectively. (in color)

ellipse in Fig. 4a leads to $\pi/2$ rotated and further stretched one in Fig. 4b, whereas the transformation (4.4) restored original orientation of the ellipse (and again stretches it) in Fig. 4c.

The equation (4.1) gives the band structure shown in Fig. 5a. The band structure of the graphene model is symmetric in respect to electrons and holes. Dispersion law for 2D-graphene in the vicinity of Dirac point $K_A(K_B)$ of Brillouin zone is linear in this model, and appropriate valent band and conductivity bands have the form of cones called Dirac cones. Due to relation $(\Sigma^x_{rel})_{BA} \neq (\Sigma^x_{rel})_{AB}$, the vector of the Dirac cone axis is somehow rotated in respect to the vector $\vec{p}_{AB}$ of its replica and respectively, the equations of motion for holes and electrons in graphene are asymmetric ones. Such a band structure is stipulated by the rotation of hole (electron) Dirac cone in respect to electron (hole) one as schematically shown in Fig. 5b.

Original electron Hamiltonian $H^{(1)}_{AB}$ is given by eq. (4.1). Similar formula for hole Hamiltonian is obtained from (4.1) by the replacement BA $(AB) \rightarrow AB$ (BA). Hamiltonians obtained under the action of transformations (4.2, 4.3) have
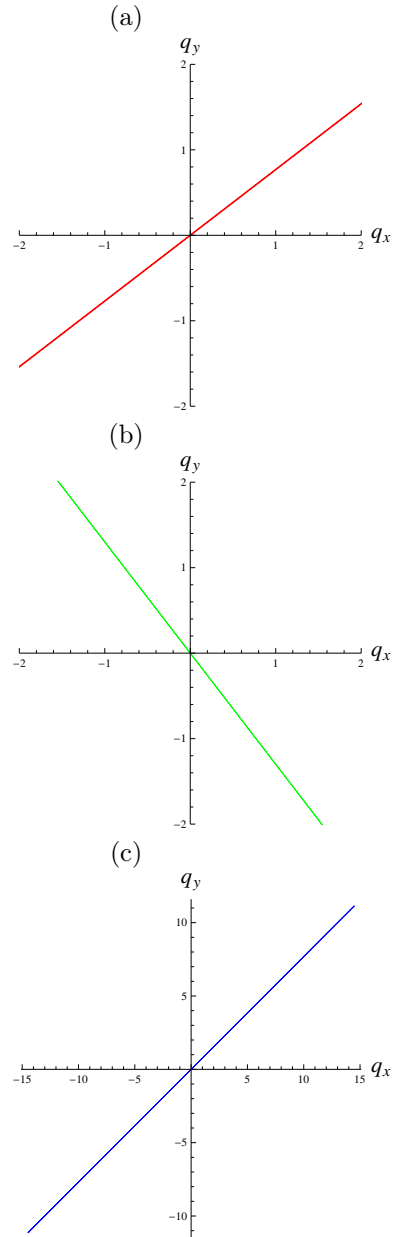

FIG. 4. Sequence of transformations of circumference by exchange operators. (in color)

the form

$$H^{(2)}_{AB} = (\Sigma^x_{rel})_{AB} \; H^{(1)}_{AB} \, (\Sigma^x_{rel})^{-1}_{AB}, \qquad (4.5)$$

$$H^{(3)}_{AB} = (\Sigma^x_{rel})_{BA} \; H^{(2)}_{AB} \, (\Sigma^x_{rel})^{-1}_{BA}. \qquad (4.6)$$

Now, we look at the action of the exchange operator applied to sum of electron and hole Dirac
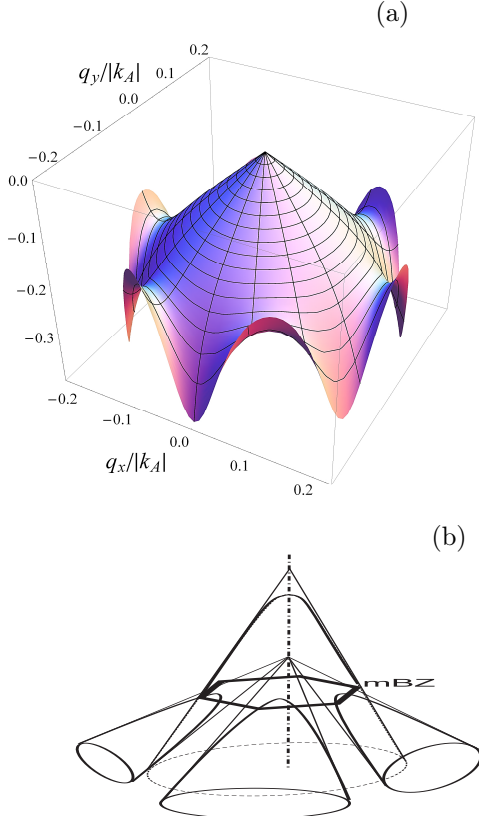
(a)

(b)

FIG. 5. (a) Partially degenerated Dirac cone in the vicinity of $K_A(K_B)$-point in graphene Brillouin zone. (b) Scheme of mini Brillouin zone (mBZ) formed due to rotation of Dirac cone replicas in respect of its apex. Three replicas of six are shown. (in color)

bands

$$c\left(E_{qu}^{e\,(1)}(p^e) + E_{qu}^{h\,(1)}(p^h)\right),\ E_{qu}^{(1)} \equiv E_{qu} \quad (4.7)$$

where $p^h = S(\phi)p^e$, $S(\phi)$ is 2D rotation matrix, $\phi = \pi/2$ in accord with above discussed. The sum of eigenvalues of transformed Hamiltonians $H^{e(2)}, H^{h(2)}$ is given by

$$c\left(E_{qu}^{e\,(2)}(p^e) + E_{qu}^{h\,(2)}(S(\phi)p^h)\right), \quad (4.8)$$

and for the transformed Hamiltonians $H^{e(3)}, H^{h(3)}$ as

$$c\left(E_{qu}^{e\,(3)}(p^e) + E_{qu}^{h\,(3)}(S(\phi)S(\phi))p^h)\right). \quad (4.9)$$

The original sum (4.7) is shown in Fig. 6a. Provided accounting for the fact that $\vec{\sigma}_{AB} \cdot \vec{p}_{BA}$ is

a helicity operator, the action of $(\Sigma_{rel}^x)_{BA}$ can be viewed as non-equilibrium transition of a carrier into a state of same pseudo-spirality, and doubled action as non-equilibrium forth and back jump. The appropriate Fig. 6b demonstrates that at the transformation (4.5), the vicinity of Dirac point gains a hyperbolic saddle point (compare the insert in Fig. 6b with the insert in Fig. 6a) and that the exchange operator action given by (4.6) leads practically to the same band structure (Fig. 6c). This allow us to investigate the influence of substrate as an additional exchange interaction.

5. Results and discussion

Let us consider van der Waals heterostructures consisting of graphene monolayers and boron nitride layer or Ir(1,1,1) one, which have similar to graphene crystallographic parameters [32].

The effects of charge carriers asymmetry in graphene stipulate the existence of charge areas of not annihilated electrons and holes. This asymmetry of charge carriers in graphene leads to appearance of hyperbolic states having the steady state of saddle type on the boundary of the regions with different types of charge carriers in accordance with Fig. 6a. Hyperbolic set with steady state saddle points [33] separates a set of energy levels of finite motion of localized electrons and holes upon the levels of infinite motion of delocalized electrons and holes. Charge carriers could stay an infinitely long within the hyperbolic set.

In the superlattice there exists an additional exchange between electrons in graphene and electrons of other non-graphene layers. As it was pointed out in previous section, in our model the exchange interaction rotates the spin and momentum of excitons and additional exchange Σ_{BA}^{ad} will rotate them additionally. In this case, as we see, the exchange can lead to the loss of stability of the Dirac point K_A, that favors the appearance of additional direct valley current $\Delta j_{v,\,BA}^{add}$. Additional exchange Σ_{AB}^{ad} will restore the electron density distribution generating additional reverse valley current $\Delta j_{v,\,AB}^{add}$. In
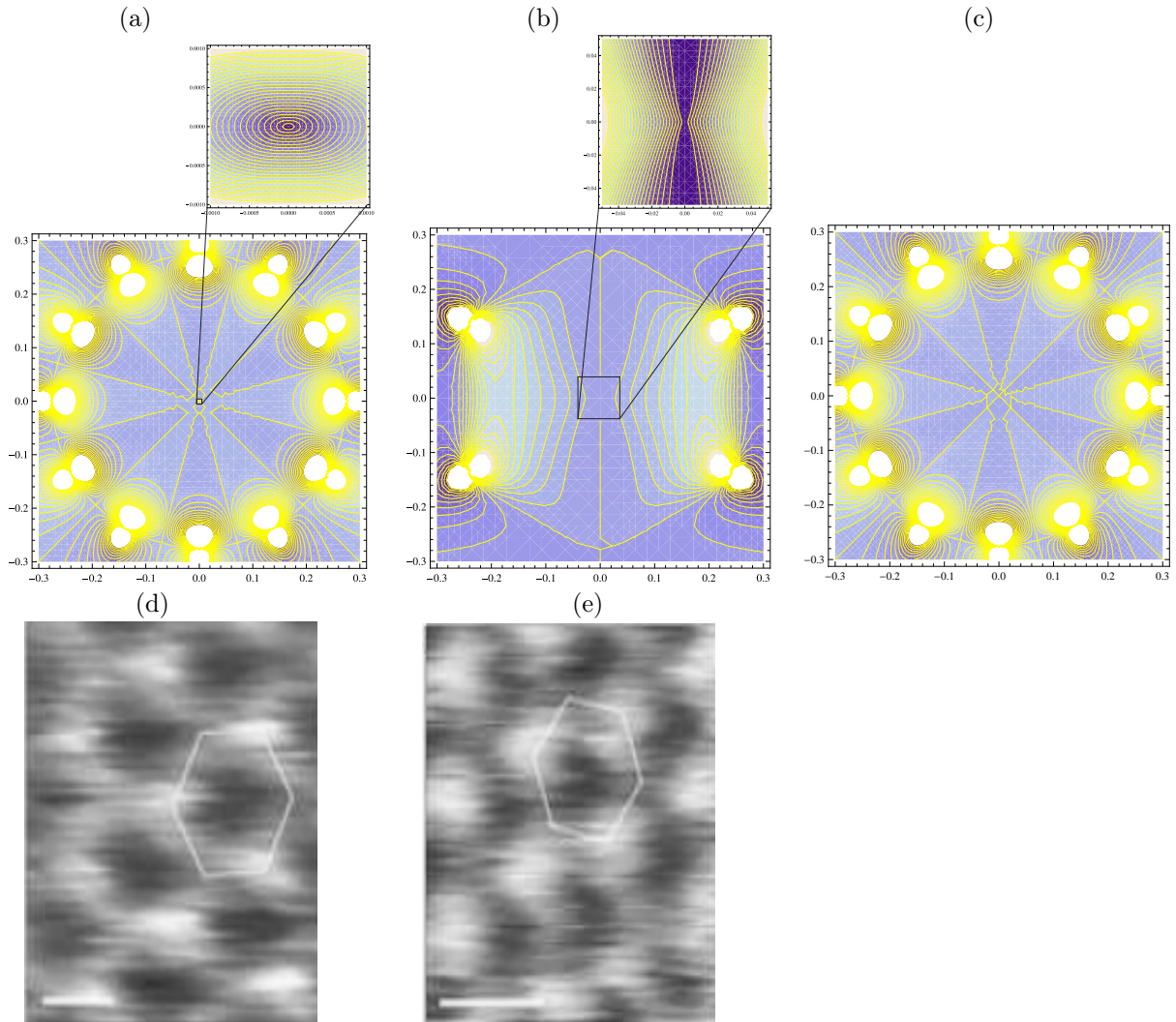
FIG. 6. Action of exchange operators on the sum of electron and hole original and transformed Dirac bands. (a) Sum of original bands, (b) single action of $(\Sigma^x_{rel})_{BA}$, (c) action of exchange operators product $(\Sigma^x_{rel})_{AB} (\Sigma^x_{rel})_{BA}$ restoring the system. Insert in (a) demonstrates that the steady state point in $K_A(K_B)$ is of center type. Insert in (b) shows an occurrence of a saddle point. (d, e) "Moire" pattern of AFM image experimentally observed in [34] for: (d) ideal heterostructure, (e) crystal lattices of two heterostructure layers are rotated on a small angle in respect to each other. (in color)

graphene, the direct and reverse valley currents compensate each other. Due to mismatch of crystal lattices we have $\Delta j^{add}_{v, BA} + \Delta j^{v, add}_{AB} \neq 0$, and therefore graphene gains additional charge ΔQ.

In accordance with Fig. 6a on distances $q_{moire} = \{q^{moire}_x, q^{moire}_y\} \approx \{0.06K_A, 0.06K_A\}$ and more from the Dirac point $K_A(K_B)$, density of localized states increases greatly

and when approaching to this point the density of hyperbolic set increases. Therefore ΔQ with larger probability is redistributed in the vicinity of saddle type hyperbolic points. In the regions of finite motion charge carriers have some pseudo-angular momentum. Contrary to this, for free charge carriers the value of this momentum is zero. Therefore, in spite of instability of saddle points, the angular momentum conservation law forbids the

transition of delocalized charge carriers into regions of finite motion and, respectively charge distribution ΔQ over hyperbolic set is stable.

The period q^{moire} in the space of inverse lattice corresponds to a period $\lambda^{moire} = 2\pi/q_{moire} \sim 2\pi a/0.06 = 15.8$ nm of electron density distribution in real 2D-space of monolayer. Here $a = 1.44$ Å is a distance between nearest C atoms. This numerically simulated effect of electron density redistribution has a form of "moire" pattern in Fig. 6a. The described process of "moire" pattern appearance is a dynamic one. The electron density in periodic potential of substrate periodically undergoes the sequence of impacts: $\{\Sigma_{AB}\Sigma_{AB}^{ad} \equiv \Sigma'_{AB} \approx \Sigma_{AB},\ \Sigma'_{BA},\ \Sigma'_{AB}\}$, returning to distribution only slightly different from original one shown in Fig. 6a.

If the potential of the substrate deviates slightly from the periodic one, the angle of rotation due to the exchange can increase, e.g., as $\Sigma_{BA}^{ad}\Sigma_{AB} \equiv \Sigma'_{BA} \approx \Sigma_{BA}$. Due to the fact that now the sequence of impacts: $\{\Sigma'_{BA},\ \Sigma'_{AB},\ \Sigma'_{BA}\}$ is finished on the additionally rotated exchange Σ'_{BA}, leading to stability break of the Dirac point K_A, in this case the electron density distribution restores periodically with rhombic symmetry which one can see in Fig. 6b. All the rest cases are related to situations when the angle of rotation in graphene and total angle of exchange stipulated rotation both in graphene and substrate are incommensurable. Because of incommensurate of phases for natural oscillations of the system and external shocks electron density distribution does not restore. The consequence of this incommensurability is a chaotical perturbation of the electron density distribution in graphene, and, respectively, the "moire" pattern is absent.

"Moire" pattern was observed experimentally in [35, 36]. The numerically calculated period $\lambda^{moire} \sim 15.8$ nm is near to experimentally measured period 15±1 nm of "moire" pattern [34] at coincidence of direction of crystallographic axes ($\theta = 0$) in superlattice graphene/BrN. Here θ is the angle of rotation of crystallographic axes of graphene and BrN lattices.

As one can see from comparison of Figs. 6a, b and Figs. 6d, e, respectively, theoretical and experimental patterns of electron density in ideal superlattice and superlattice with very small misalignment of crystal lattices are coincided. For very small rotation angle of the crystal axes of superlattice layers relative to each other, the theory predicts a rhombic "moire" , which is observed experimentally (see Atomic Force Microscopy (AFM) image in Fig. 6e). For ideal superlattice the theory predicts hexagonal "moire" , which is also observed in experiment (AFM-image in Fig. 6d).

Stability loss of a spin-flip state in the model $N = 3$

In this section we propose a mechanism of reorientation of the spin of the electron density in graphene by magnetic scatterers, which can explains the large spin relaxation times in the graphene monolayers.

External hits exerted on a graphene electronic subsystem by external magnetic impurities through exchange interactions, formally are resulted into transition from one moving reference frame into another, rotated relative to the first via transformation $\Sigma_{rel,\ adm}^x$. Let us denote an impurity magnetization vector through $\vec{M}^{adm}$.

According to the results obtained, the exchange interaction provides two kind of rotations for spin $\vec{\sigma}_{AB}$ and for momentum $\vec{p}_{BA}$ of charged exciton. The first kind of rotations gives the following condition for rotation at small angle: $\Sigma_{nf}^x \equiv \Sigma_{rel,\ adm}^x\Sigma_{AB}^x \approx \Sigma_{AB}^x$. The second kind of rotation gives the condition of approximate equality of the total angle of rotation performed by sequence of k_{flip} magnetic scatterers, to the angle of rotation, performed by exchange interaction Σ_{BA}^x: $\sum_{i=1}^{k_{flip}} \Sigma_{nf_i}^x \equiv \Sigma_{flip}^x \approx \Sigma_{BA}^x$. Exchange Σ_{nf}^x creates a nonequilibrium valley current with an orbital angular momentum $\vec{L}_{AB}$ and precessing spin $\vec{\sigma}'_{AB} = \Sigma_{nf}^x\vec{\sigma}\left(\Sigma_{nf}^x\right)^{-1}$. The emerging total magnetic moment $\vec{J}_D = \vec{\sigma}' + \vec{L}_{AB}$ tends to compensate the vector of the impurity magnetic susceptibility $\vec{M}^{adm}$: $\vec{J}_D = -\vec{M}^{adm}$.

Exchange Σ_{flip}^x leads to instability of those

states, which spin could carry flip. Due to instability of $\Sigma_{flip}^x \vec{\sigma}_{AF} \left(\Sigma_{flip}^x \right)^{-1}$ only narrowing of the spin distribution of states of graphene occurs, rather than their magnetic ordering. As a consequence, in ideal situation this means that the time of spin relaxation increases indefinitely.

Thus, the mechanism of instability of spin-flip states in graphene has been proposed.

6. Conclusion

Let we summarize our findings. A model of graphene with the number of internal degrees of freedom $N = 3$ has been proposed, in which charge carriers are charged excitons. It is shown that in this model there exists mechanism of dynamic reductions of spatial dispersion of state and narrowing of the distribution of spin states. This dynamic reduction provides longer duration of the pseudo-spin rotation caused by exchange with external magnetic scatterers. Peculiarities of this process in graphene has been established. They consist in generation of additional valley currents and hence of magnetic magnetization that compensates vector of impurity magnetization without loss of stability of the charge carrier spin state. A condition is found under which the spin flip occurs.

References

[1] P.J.Zomer, M.H.D. Guimarres, N. Tombros, B. J. van Wees. Longdistance spin transport in high-mobility graphene on hexagonal boron nitride. Phys. Rev. B **86**, 161416 (2012).

[2] Wei Han, R.K. Kawakami, M. Gmitra, Ja. Fabian. Graphene spintronics. Nature Nanotechnology. **9**, 794–807 (2014).

[3] R.J. Elliott. Theory of the effect of spin–orbit coupling on magnetic resonance in some semiconductors. Phys. Rev. **96**, 266–279 (1954).

[4] Y.Yafet. In: *Solid State Physics*. Eds. F.Seitz, D. Turnbull. Vol. 14. (Academic, 1963). Pp.1–98.

[5] D.Kochan, M.Gmitra, J.Fabian. Spin relaxation mechanism in graphene: resonant scattering by magnetic impurities. Phys. Rev. Lett. **112**, 116602 (2014).

[6] K.S. Novoselov, A.K. Geim, S.V. Morozov, D.Jiang, Y. Zhang, M.I. Katsnelson, I.V. Grigorieva, S.V. Dubonos, A.A. Firsov. Two-dimensional gas of massles Dirac fermions in graphene. Nature. **438**, 197 (2005).

[7] N.M.R. Peres. The transport properties of graphene. J. Phys. Condens. Matter. **21**, 323201 (2009).

[8] Y. Hancock. The 2010 Nobel Prize in physics—ground-breaking experiments on graphene // J. Phys. D. – 2011. – V. 44. – P. 473001.

[9] O. Klein. Die Reflexion von Elektronen an einem Potentialsprung nach der relativistischen Dynamik von Dirac. Z. Phys. **53**, 157–165 (1928).

[10] B. Thaller. Normal forms of an abstract Dirac operator and applications to scattering theory. J. Math. Phys. **29**, 249–257 (1988).

[11] M.I. Dyakonov, V.I. Perel. Spin relaxation of conduction electrons in noncentrosymmetric semiconductors. Sov. Phys. Solid State **13**, 3023–3026 (1972).

[12] S.V. Kryuchkov, E.I. Kukhar. Influence of the magnetic field on the graphene conductivity. J.Mod.Phys. **3**, 994-1001 (2012).

[13] D.S.L. Abergel, V. Apalkov, J. Berashevich, K. Ziegler, T. Chakraborty. Properties of graphene: a theoretical perspective. Advances in Physics. **59**, 261 (2010).

[14] J.Z. Bernád. Optical conductivity of single-layer graphene induced by temporal mass-gap fluctuations. Physica B. **407**, 4446 (2012).

[15] L.A. Falkovsky, A.A. Varlamov. Space-time dispersion of graphene conductivity. Eur. Phys. J. B. **56**, 281 (2007).

[16] V.P. Gusynin, S.G. Sharapov, J.P. Carbotte. AC conductivity of graphene: from tight-binding model to 2 + 1-dimensional quantum electrodynamics. Int. J. Mod. Phys. B. **21**, 4611-4658 (2007).

[17] Jing-Rong Wang, Guo-Zhu Liu. Eliashberg theory of excitonic insulating transition in graphene. J. Phys.: Condens. Matter. **23**, 155602 (2011).

[18] G.W. Semenoff. Condensed-matter simulation of a three-dimensional anomaly // Phys. Rev. Lett. – 1984. – V. 53. – P. 2449.

[19] H.V. Grushevskaya, G. Krylov. Quantum Field Theory of Graphene with Dynamical Partial Symmetry Breaking. Journal of Modern Physics. **5**, 984-994 (2014).

[20] M.E. Peskin, D.V. Schroeder. *An Introduction to Quantum Field Theory.* (Addison–Wesley Publishing Company, 1995).

[21] V.N. Gribov. Quantum Electrodynamics. (R & C Dynamics, Izhevsk, 2001).

[22] V.A. Fock. *Principles of quantum mhechanics.* (Science, Moscow, 1976).

[23] H. Eschrig, M. Richter, I. Opahle. Relativistic Solid State Calculations. In: *Relativistic Electronic Structure Theory*, part 2. Applications. Ed. P. Schwerdtfeger. Theor. and Comput. Chem. Vol. 13. (Elsevier, 2004); I. Opahle, M. Koepernik, R.H. Eschrig. Relativistic code. FPLO. – 2008. – at http://www.fplo.de/workshop/ws2008/rfplo08.pdf

[24] G.G. Krylov, H.V. Krylova, M.A. Belov. Electron transport in low dimensional systems with non-trivial topology: effects of localization. *Dynamical phenomena in complex systems.* Eds. A.V. Mikshin *et al.* (MOiN RT Publisher, Kazan, 2011). Pp.161–180.

[25] H.V. Grushevskaya, G.G. Krylov. Charge Carriers Asymmetry and Energy Minigaps in Monolayer Graphene: Dirac—Hartree–Fock approach. J. Nonlin. Phenom. in Complex Sys. **16**, 189 (2013).

[26] H.V. Grushevskaya, G.G. Krylov. Partially Breaking Pseudo-Dirac Band Symmetry in Graphene // Int. J. Nonlin. Phen. in Complex Sys. **17**, 86 (2014).

[27] H.V. Grushevskaya, G.G. Krylov. Graphene: Beyond the Massless Dirac's Fermion Approach. In: *Nanotechnology in the Security Systems.* Eds. J. Bonča, S. Kruchinin. (Springer Science+Business Media, Dordrecht, 2015). Pp. 21-31. DOI 10.1007/978-94-017-9005-5-3.

[28] H.V. Krylova. *Electric charge transport and nonlinear polarization of periodically packed structures in strong electromagnetic fields.* (Publishing Center of BSU, Minsk, 2008).

[29] Halina Krylova, Leonid Hursky. *Spin polarization in strong-correlated nanosystems.* (LAP LAMBERT Academic Publishing, AV Akademikerverlag GmbH & Co., Germany, 2013).

[30] H.V. Grushevskaya, L.I. Hurskiy. Polarization effects of many-electron atom in electron–hole formalizm. Report of BSUI& R. No. 3, 5-17 (2007).

[31] G.V. Grushevskaya, L.I. Gursky, P.N. Luskinovich, I.A. Lubashevskii. Effects of Spatial Distribution of the Electron Density Functional in Crystals. Bulletin of the Lebedev Physics Institute. **34**, 127-134 (2007).

[32] C.R. Dean, A.F. Young, I. Meric. Boron nitride substrates for high-quality graphene electronics // Nature Nanotechnology. **5**, 722 (2010).

[33] I.A. Kovalew, D.W. Serow. Illustrations of Irreducibility and Tops of Umbrellas in the PostScript Methodology. J.Nonlin. Phenom. in Complex Sys. **17**, 318–326 (2014).

[34] Zhi-Guo Chen, Zhiwen Shi, Wei Yang, Xiaobo Lu, You Lai, Hugen Yan, Feng Wang, Guangyu Zhang, Zhiqiang Li. Observation of an intrinsic bandgap and Landau level renormalization in graphene/boron-nitride heterostructures. Nature Communications. **5**, 4461 (2014) DOI: 10.1038

[35] I. Pletikosic, M. Kralj, P. Pervan, R. Brako, J.Coraux, A. T. N'Diaye, C. Busse, T. Michely. Dirac Cones and Minigaps for Graphene on Ir(111). Phys. Rev. Lett. **102**, 056808 (2009), arXiv: 0807.2770v2 [cond-mat.mtrl-sci] 13 Feb2009.

[36] C. R. Woods, L. Britnell, A. Eckmann, R. S. Ma, J. C. Lu, H. M. Guo, X. Lin, G. L. Yu, Y. Cao, R. V. Gorbachev, A. V. Kretinin, J. Park, L. A. Ponomarenko, M. I. Katsnelson, Yu. N. Gornostyrev, K. Watanabe, T. Taniguchi, C. Casiraghi, H-J. Gao, A. K. Geim, K. S. Novoselov. Commensurate–incommensurate transition in graphene on hexagonal boron nitride. Nature Physics. **10**, 451-456 (2014). doi:10.1038/nphys2954